Supporting information for: Morphology of Anion-Conducting Ionenes Investigated by X-ray Scattering and Simulation

Eric M. Schibli,[†] Andrew G. Wright,[‡] Steven Holdcroft,[‡] and Barbara J. Frisken*[,†]

[†]*Department of Physics, Simon Fraser University, Burnaby BC Canada V5A 1S6*

[‡]*Department of Chemistry, Simon Fraser University, Burnaby BC Canada V5A 1S6*

E-mail: frisken@sfu.ca

Molecular Dynamics Simulations

The molecular model is shown in Fig. S1.

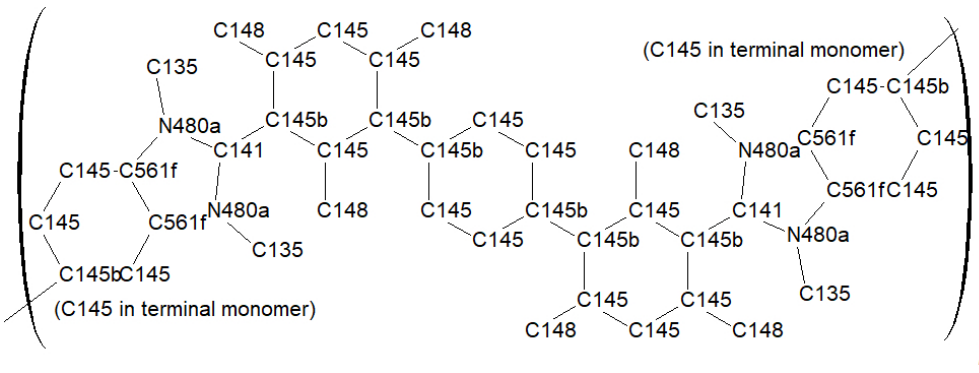

Figure S1: A monomer of 100% dm HMT-PMBI, labeled with the atom types. Hydrogens are excluded from this figure. Hydrogens in the methyl groups bonded to nitrogen are labeled H911, those in methyl groups bonded to carbon are labeled H140, and those bonded to aromatic carbons are labeled H146.

We used the Optimized Parameters for Liquid Simulations - All Atoms (OPLS-AA) force field distributed with NAMD 2.11 for the MD simulations,[S1] where available. Non-bonded parameters for iodide were taken from Ref. S2, and the final eight dihedral parameters, related to twisting between benzimidazolium and mesitylene groups and to twisting between the benzimidazolium methyl groups, were taken from the CHARMM general force field.[S3] The parameters we used are tabulated in Tables S1, S2 and S3.

Atomic partial charges for the simulation were assigned according to the CHELPG (CHarges from Electrostatic Potentials using a Grid-based method) scheme, in which the atomic charges are fit to the molecular electrostatic potential on a 3 pm rectangular grid of points surrounding the molecule.[S4] This charge distribution is depicted in Fig. S2. This procedure was used to produce partial charges in a recent simulation of acid-doped PBI.[S5] The grid excludes points within the van der Waals radius of any atom, and includes 28 pm of extra space around the molecule in each dimension. This represents a second departure from the procedure of Ref. S6, in which the atomic charges of each accessible atom are fit to the atom's interaction energies with water. This would also have been very expensive,

Table S1: OPLS-AA bond-stretching parameters for 100% dm HMT-PMBI(I^-).

Atom	Atom	K_r (kcal/mol/Å^2)	r_0 (Å)
C141	C145	392.00	1.400
C141	N480a	375.000	1.365
N480a	C561f	375.000	1.365
N480a	C135	320.000	1.448
C561f	C561f	392.00	1.400
C561f	C145	392.00	1.400
C145	C145B	392.00	1.400
C145	H146	307.000	1.080
C145B	C145B	392.00	1.400
C145	C145	392.00	1.400
C135	H911	285.00	1.090
C145	C148	365.00	1.510
C148	H140	340.000	1.090
OT	HT	450.0	0.9572
HT	HT	0.0	1.5139

and unlikely to give good results, as the most highly charged atoms in HMT-PMBI are not accessible to water.

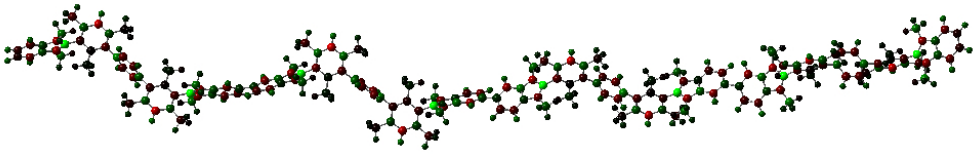

Figure S2: Atomic partial charges. Green nuclei were assigned more positive charges; red nuclei, negative charges. The bulk of the charge appearing in the apex carbon of the imidazole ring is in agreement with an investigation of similar materials in Ref. S7.

Molecular dynamics simulations were performed using NAMD 2.10.[S8] **The initial configuration of the 25 tetramers was produced using Packmol.[S9]** The energy was then minimized using a conjugate-gradient algorithm, and the cell was annealed at 1000 K for 1 ns at constant volume. The cell size was then reduced to $80 \times 80 \times 80$ Å^3 (representing a density of 0.35 g/ml), periodic boundaries were added, and the system was then cooled to 800 K and annealed for a further 20 ns at constant pressure (1 atm). **Subsequently, water and counter-ions were added, again using Packmol, and the system was**

Table S2: OPLS-AA angle-bending parameters for 100% dm HMT-PMBI(I^-).

Atom	Atom	Atom	K_θ (kcal/mol/rad^2)	θ_0 (°)
C141	N480a	C135	70.00	125.000
C141	N480a	C561f	70.00	125.000
N480a	C561f	C145	70.00	108.000
N480a	C561f	C561f	70.00	108.000
N480a	C141	C145	70.00	108.000
N480a	C141	N480a	70.00	123.000
N480a	C135	H911	35.00	109.000
C561f	C145	H146	35.00	109.500
C561f	N480a	C135	50.00	118.000
C145	C148	H140	33.00	109.500
C145	C145	C148	70.00	120.000
C145B	C145	C148	70.00	120.000
C145B	C145	H146	35.00	109.500
C145	C145	H146	35.00	120.000
H140	C148	H140	33.00	107.800
H911	C135	H911	33.00	107.800
C561f	C145	C145	63.00	120.000
C145B	C145	C145	63.00	120.000
C145	C145B	C145B	63.00	120.000
C145	C145B	C145	63.00	120.000
C141	C145	C145	63.00	120.000
C561f	C145	C145B	63.00	120.000
C561f	C561f	C145	63.00	120.000
C145	C145	C145	63.00	120.000
HT	OT	HT	55.0	104.52

energy-minimized and annealed at 500 **K for an additional** 20 **ns at** 1 **atm,** and then cooled to 298 K in 1 K, 5 ps steps. To prevent large temperature gradients from appearing during the cooling phase, velocities were reassigned to match the thermostat temperature at each step. Finally, the cell was equilibrated for 50 ns, and sampling was performed over an additional 150 ns of simulation. Constant pressure simulations were performed via the Noosé-Hoover Langevin piston method,[S10] using periodic boundary conditions. The relaxation time was set to 0.2 ps, the damping coefficient was set to 5 ps^{-1}, and the integration timestep was set to 1 fs, the default values in NAMD.

Pair-Correlation Functions

Pair-correlation functions describe the probability of finding a particle at a distance r from a reference particle. We used pair-correlation functions to provide insight into the origins of the three length scales visible in the scattering profiles. Results for pair-correlation functions calculated using VMD[S11] for the equilibrated simulation cells are shown in Fig. S3. **Calculations included correlations between iodide ions and carbon and nitrogen atoms (iodide-backbone), between oxygen atoms and carbon and nitrogen atams (water-backbone), between carbon and nitrogen atoms that are not members of the same chain (backbone-backbone), between water and iodide, and between members of imidazole rings in the same chain (imidazole-imidazole). Hydrogen atoms were not considered in this calculation because they do not contribute meaningfully to the scattering. The pair-correlation functions are not weighted by scattering cross-sections.** The results were averaged over the sampling phase. **Iodide-polymer and water-polymer are shown as one curve because the two correlation functions are similar. The results show that length scales associated with Peaks 0, 1 and 2 from the calculated structure factor, as labeled in Fig. S3, correspond to either a peak or a shoulder in the pair-correlation functions. In Figs. S3 (a) and (b), the correlation structure associated with iodide-backbone, water-backbone and iodide-water curves corresponds to the location of Peak 2, while the correlation structure associated with the backbone-backbone curve corresponds to the location of Peak 1, as identified on the figure. The first peak in Figs. S3 (c) and (d) corresponds to spacing between adjacent imidazole rings, while the peak at approximately 20 Å corresponds to the monomer-monomer spacing.**

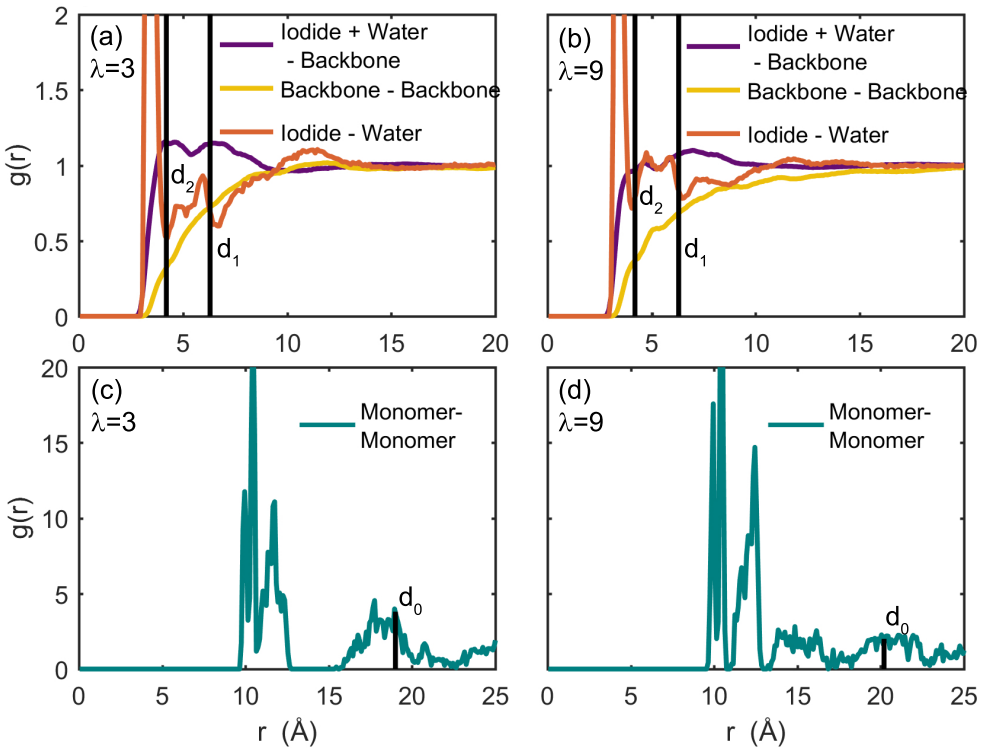

Figure S3: Results for pair-correlation functions calculated from the MD simulations for the $\lambda = 3$ cell are shown in (a) and (c) while results for the $\lambda = 9$ cell are shown in (b) and (d). Results for the iodide- and water-backbone and backbone-backbone correlations are shown in the top row (a and b), while results for monomer-monomer correlations are shown in the bottom row (c and d). The length scales estimated from scattering measurements of comparable samples are shown as black bars.

Cluster Analysis

A cluster analysis was performed to confirm that the water and ions formed a percolating network in our simulation results, similar the technqiue used in.[?] Atoms within 3 Åwere considered to be part of the same cluster. The results were averaged over 100 frames separated by 1.5 ns. The results are shown in Figs. S4 and S5.

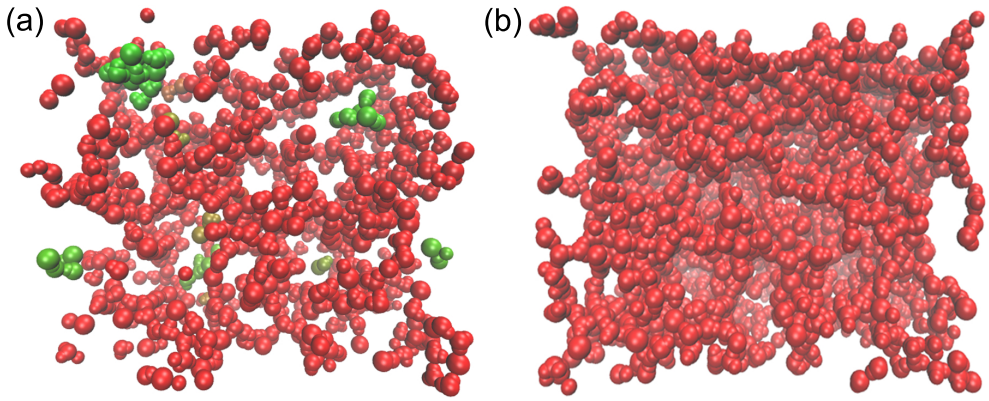

Figure S4: **Results for cluster-analysis calculations performed on the MD simulations at (a) $\lambda = 3$ and (b) $\lambda = 9$. Iodide ions, water oxygens, and water hydrogens are shown as spheres of their van der Waals radii. The percolating network is shown in red, while particles that are isolated or part of smaller clusters are shown in green.**

Small-Angle Neutron Scattering

Exploratory small-angle neutron scattering (SANS) experiments were performed by our collaborator, Dr. Sandrine Lyonnard, at the Labratoire Léon Brillouin (Saclay, France). Samples were hydrated in either H_2O or D_2O to take advantage in the very different scattering lengths of protium and deuterium. Results for three HMT-PMBI(I^-) samples with dm = 65.9, 80.2 and 89.7 % are shown in Fig. S6. The data show a smooth transition from a power law at low q to a flat background at higher q when hydrated with either H_2O or D_2O. There are no peaks, knees, or other features associated with phase separation, consistent with the SAXS results for the same q-range. The vertical shift in the H_2O data relative to the D_2O data for the higher-IEC samples reflects the higher level of incoherent scattering by H_2O.

Analysis

As the form factor of the scatterers is not known a priori, we have selected a fitting function that combines a sum of three pseudo-Voigt functions—each a sum of a Gaussian and

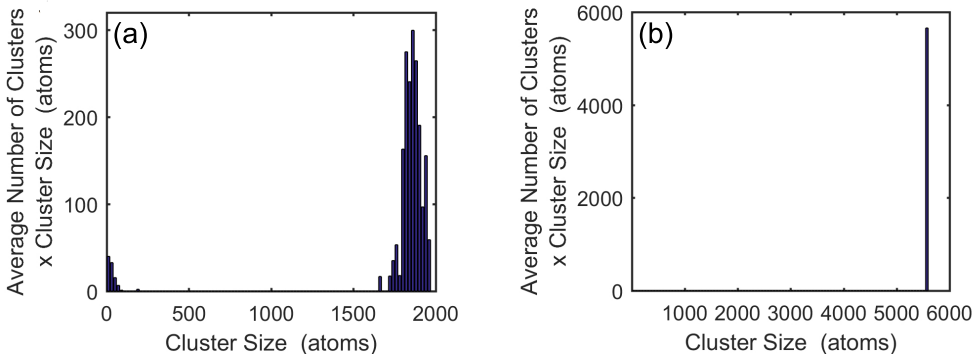

Figure S5: **The results of the culster-analysis calculation showing the cluster size distribution for 100 frames of the MD simulation. The x-axis shows cluster size, while the y-axis shows average number of clusters of a given size, multiplied by the size of the clusters, in order to compare the distribution of atoms. (a) Results for λ=3 show that most atoms are part of a large cluster that averages 1800 atoms in size. (b) Results for λ=0 show that all atoms are part of a single cluster in each sample of the MD simulation.**

Lorentzian peak with the same positions and widths—with a single power law function with amplitude a_o and power p and a flat baseline b_o:[S12]

$$I(q) = a_o \cdot q^{-p} + \sum_i \left\{ s_i \cdot a_i \cdot \exp\left(-(2\cdot(q-b_i)/c_i)^2 \cdot \log(2)\right) + \frac{a_i \cdot (1-s_i)}{(1+(2\cdot((q-b_i)/c_i)^2))} \right\} + b_o. \quad (1)$$

Psuedo-Voigt functions provide a flexible peak shape from a minimal number of parameters. The parameters a_i, b_i, c_i, and s_i define the peak height, position, full width at half max, and shape, respectively, of each peak. Both the frequency of occurrence of a length scale and the scattering factors of the scatterers contribute to the peak intensity. While the size of crystallites may be inferred from c_i through the Debye-Sherrer formula—which states crystallite diameter is inversely proportional to peak width[S13]—as we only observed non-crystalline peaks, we did not consider peak width quantitatively; rather, we assumed a broader peak indicated a less well-defined length scale. $s_i = 1$ corresponds to a pure Gaussian peak, while $s_i = 0$, to a completely Lorentzian peak.

The mid-q feature in the 97.5% dm HMT-PMBI(Cl-) data was fit to the correlation length model as implemented in the NIST small-angle scattering

package[S14]

$$I(q) = \frac{A}{q^n} + \frac{C}{1 + (q\xi)^m} + B \quad , \tag{2}$$

where ξ is the correlation length, A and C are scale parameters, n is the exponent associated with the low-q power law, m describes the shape of the shoulder, and B is the q-independent background.

The fits were performed in three stages, each using MATLAB 2014b's weighted trust-region nonlinear least-squares fit procedure. First, the data below the first (local) intensity minimum was fit to $a_o \cdot q^p + b_o$. The result was then subtracted from the remaining data, and the difference was fit to a sum of Gaussian peaks. The resulting fit parameters were then used as a starting point to fit Equation 1 to the full range of the original data. Finally, a Monte Carlo algorithm was used to estimate the uncertainty in each fit parameter using uncertainties for each datapoint as reported by SAXSGUI. Results are tabulated in Tables S4, S5, S6, S7, S8, and S9.

Parameters determined from fits of Eq. 1 to the data

We assume that each visible peak corresponds to a single length scale in the material

$$d \;=\; 2.44 \times \frac{\pi}{q} \tag{3}$$

as recommended for broad amorphous peaks.[S15] Results are tabulated in Tables S10, S11, and S12.

References

(S1) Jorgensen, W. L.; Maxwell, D. S.; Tirado-Rives, J. Development and Testing of the OPLS All-Atom Force Field on Conformational Energetics and Properties of Organic Liquids. *J. Am. Chem. Soc.* **1996**, *118*, 11225–11236.

(S2) Jensen, K. P.; Jorgensen, W. L. Halide, Ammonium, and Alkali Metal Ion Parameters for Modeling Aqueous Solutions. *J. Chem. Theory Comput.* **2006**, *2*, 1499–1509.

(S3) Vanommeslaeghe, K.; Hatcher, E.; Acharya, C.; Kundu, S.; Zhong, S.; Shim, J.; Darian, E.; Guvench, O.; Lopes, P.; Vorobyov, I.; et al., CHARMM General Force Field: A Force Field for Drug-Like Molecules Compatible with the CHARMM All-Atom Additive Niological Force Fields. *J. Comput. Chem.* **2010**, *31*, 671–690.

(S4) Breneman, C. M.; Wiberg, K. B. Determining Atom-Centered Monopoles from Molecular Electrostatic Potentials. The Need for High Sampling Density in Formamide Conformational Analysis. *J. Comput. Chem.* **1990**, *11*, 361–373.

(S5) Zhu, S.; Yan, L.; Zhang, D.; Feng, Q. Molecular Dynamics Simulation of Microscopic Structure and Hydrogen Bond Network of the Pristine and Phosphoric Acid Doped Polybenzimidazole. *Polymer* **2011**, *52*, 881–892.

(S6) Mayne, C. G.; Saam, J.; Schulten, K.; Tajkhorshid, E.; Gumbart, J. C. Rapid Parameterization of Small Molecules Using the Force Field Toolkit. *J. Comput. Chem.* **2013**, *34*, 2757–2770.

(S7) Henkensmeier, D.; Cho, H.; Brela, M.; Michalak, A.; Dyck, A.; Germer, W.; Duong, N. M. H.; Jang, J. H.; Kim, H.-J.; Woo, N.-S.; et al., Anion Conducting Polymers Based on Ether Linked Polybenzimidazole (PBI-OO). *Int. J. of Hydrogen Energy* **2014**, *39*, 2842–2853.

(S8) Kalé, L.; Skeel, R.; Bhandarkar, M.; Brunner, R.; Gursoy, A.; Krawetz, N.; Phillips, J.; Shinozaki, A.; Varadarajan, K.; Schulten, K. NAMD2: Greater Scalability for Parallel Molecular Dynamics. *J. Comput. Phys.* **1999**, *151*, 283–312.

(S9) Martínez, L.; Andrade, R.; Birgin, E. G.; Martínez, J. M. Packmol: A package for building initial configurations for molecular dynamics simulations. *J. Comput. Chem.* **2009**, *30*, 2157–2164.

(S10) Feller, S. E.; Zhang, Y.; Pastor, R. W.; Brooks, B. R. Constant Pressure Molecular Dynamics Simulation: The LangevinPiston Method. *J. Chem. Phys.* **1995**, *103*, 4612–4621.

(S11) Humphrey, W.; Dalke, A.; Schulten, K. VMD – Visual Molecular Dynamics. *J. Mol. Graphics* **1996**, *14*, 33–38.

(S12) Rabiej, S. A Comparison of Two X-ray Diffraction Procedures for Crystallinity Determination. *Eur. Polym. J.* **1991**, *27*, 947–954.

(S13) Scherrer, P. *Kolloidchemie Ein Lehrbuch*; Springer, 1912; pp 387–409.

(S14) Kline, S. R. Reduction and analysis of SANS and USANS data using IGOR Pro. *Journal of applied crystallography* **2006**, *39*, 895–900.

(S15) Roe, R.-J. *Methods of X-Ray and Neutron Scattering in Polymer Science*; Oxford University Press, 2000.

Table S3: OPLS-AA/CHARMM dihedral-angle parameters for 100% dm HMT-PMBI(I^-).

Atom	Atom	Atom	Atom	K_ϕ (kcal/mol/rad^2)	n	Offset (°)
X	C145	C145	X	3.6250	2	180.0
X	C561f	C561f	X	3.6250	2	180.0
C141	N480a	C135	H911	0.1500	3	180.00
C561f	N480a	C135	H911	0.1500	3	180.00
C145B	C145	C148	H140	0.1500	3	180.00
C145	C145	C148	H140	0.1500	3	180.00
N480a	C561f	C145	C145B	3.6250	2	180.0
N480a	C561f	C145	H146	3.6250	2	180.0
N480a	C141	C145	C145	3.6250	2	180.0
C561f	C561f	C145	C145B	3.6250	2	180.0
C561f	C561f	C145	H146	3.6250	2	180.0
C561f	C145	C145B	C145	3.6250	2	180.0
C561f	C145	C145B	C145B	3.6250	2	180.0
C561f	C561f	C145	C145	3.6250	2	180.0
C145	C145B	C145	C145	3.6250	2	180.0
C145	C145B	C145	H146	3.6250	2	180.0
C145	C145B	C145B	C145	3.6250	2	180.0
H146	C145	C145B	C145B	3.6250	2	180.0
C145B	C145B	C145	C145	3.6250	2	180.0
C145	C145B	C145	C148	3.6250	2	180.0
C145B	C145B	C145	C148	3.6250	2	180.0
N480a	C561f	C145	C145	3.6250	2	180.0
C141	N480a	C561f	C561f	12.0000	2	180.00
C141	N480a	C561f	C145	12.0000	2	180.00
N480a	C141	N480a	C561f	12.0000	2	180.00
C145	C141	N480a	C561f	12.0000	2	180.00
N480a	C141	N480a	C135	6.0000	2	180.00
C135	N480a	C561f	C561f	6.0000	2	180.00
C135	N480a	C561f	C145	6.0000	2	180.00
C145	C141	N480a	C135	6.0000	2	180.00

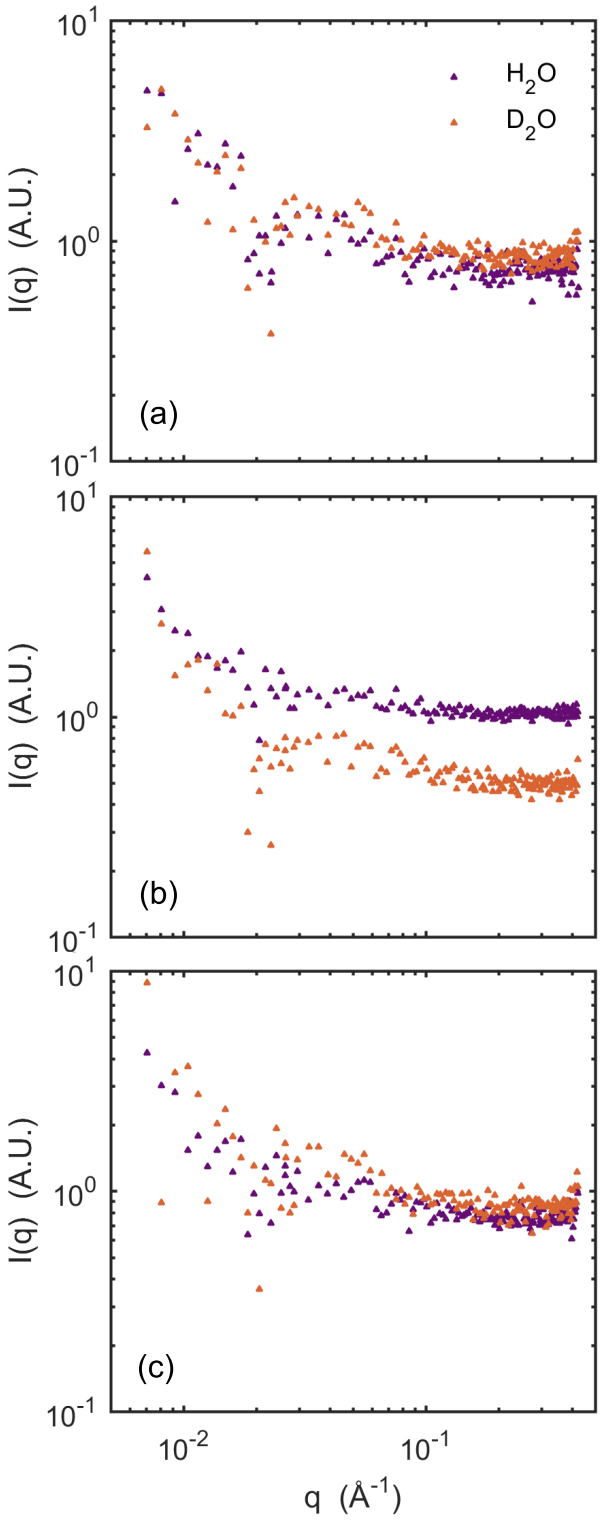

Figure S6: Small-angle neutron scattering results for the HMT-PMBI(I^-) membranes, (a) 65.9% dm, (b) 80.2%, and (c) 89.7%, plotted with logarithmic axes. These materials demonstrate a smooth transition from a power law at low q to a flat background at higher q. This is typical of amorphous polymers with no phase separation.

Table S4: Fit parameters for HMT-PMBI(I^-), measured in vacuum.

	97.5% dm	89.7% dm	80.2% dm	65.9% dm
a_1	$(4.9 \pm 0.4) \times 10^{-4}$	$(4.2 \pm 0.4) \times 10^{-4}$	$(3.9 \pm 0.4) \times 10^{-4}$	$(1.9 \pm 0.3) \times 10^{-4}$
b_1	0.429 ± 0.003	0.425 ± 0.005	0.406 ± 0.004	0.38 ± 0.01
c_1	0.43 ± 0.03	0.39 ± 0.04	0.38 ± 0.03	0.29 ± 0.04
s_1	0.1 ± 0.2	0 ± 0.3	0 ± 0.3	1 ± 0.4
a_2	$(2.7 \pm 0.2) \times 10^{-3}$	$(1.9 \pm 0.1) \times 10^{-3}$	$(2.2 \pm 0.1) \times 10^{-3}$	$(1.93 \pm 0.03) \times 10^{-3}$
b_2	1.365 ± 0.003	1.337 ± 0.002	1.319 ± 0.004	1.268 ± 0.003
c_2	0.76 ± 0.02	0.63 ± 0.02	0.69 ± 0.02	0.611 ± 0.008
s_2	0.11 ± 0.04	0.42 ± 0.08	0.38 ± 0.04	0.7 ± 0.06
a_3	$(2.24 \pm 0.09) \times 10^{-3}$	$2.3 \pm 0.1 \times 10^{-3}$	$(1.69 \pm 0.06) \times 10^{-3}$	$(9.6 \pm 0.4) \times 10^{-4}$
b_3	2.103 ± 0.008	2.05 ± 0.01	2.07 ± 0.01	1.959 ± 0.008
c_3	0.82 ± 0.07	1.11 ± 0.07	0.84 ± 0.06	0.83 ± 0.04
s_3	1.0 ± 0.3	0 ± 0.3	1 ± 0.2	0.6 ± 0.2
a_o	$(8 \pm 2) \times 10^{-9}$	$(3 \pm 3) \times 10^{-9}$	$(3 \pm 1) \times 10^{-9}$	$(1.0 \pm 0.5) \times 10^{-8}$
p	-3.43 ± 0.07	-3.5 ± 0.2	-3.68 ± 0.07	-3.4 ± 0.1
b_o	$(1.66 \pm 0.05) \times 10^{-3}$	$(1.74 \pm 0.06) \times 10^{-3}$	$(1.88 \pm 0.04) \times 10^{-5}$	$(2.2 \pm 0.5) \times 10^{-4}$

Table S5: Fit parameters for HMT-PMBI(Cl^-), measured in vacuum.

	97.5% dm	89.7% dm	80.2% dm	65.9% dm
a_1	$(2.8 \pm 0.2) \times 10^{-4}$	$(8.0 \pm 0.5) \times 10^{-4}$	$(7.1 \pm 0.4) \times 10^{-4}$	$(7 \pm 1) \times 10^{-4}$
b_1	0.416 ± 0.003	0.386 ± 0.003	0.383 ± 0.003	0.350 ± 0.005
c_1	0.23 ± 0.01	0.32 ± 0.01	0.31 ± 0.01	0.38 ± 0.05
s_1	1 ± 0.3	1.0 ± 0.1	1.0 ± 0.2	1.0 ± 0.3
a_2	$(3.2 \pm 0.1) \times 10^{-3}$	$(4.6 \pm 0.1) \times 10^{-3}$	0.0044 ± 0.0001	$(4.41 \pm 0.06) \times 10^{-3}$
b_2	1.280 ± 0.003	1.197 ± 0.004	1.179 ± 0.003	1.179 ± 0.003
c_2	0.764 ± 0.007	0.749 ± 0.007	0.721 ± 0.007	0.733 ± 0.008
s_2	0.69 ± 0.04	1.00 ± 0.02	0.96 ± 0.03	0.80 ± 0.06
a_3	$(2.23 \pm 0.05) \times 10^{-3}$	$(1.86 \pm 0.06) \times 10^{-3}$	$(1.29 \pm 0.06) \times 10^{-3}$	$(7 \pm 1) \times 10^{-4}$
b_3	2.03 ± 0.01	2.02 ± 0.01	1.99 ± 0.01	1.95 ± 0.01
c_3	0.98 ± 0.05	0.78 ± 0.06	0.75 ± 0.08	0.60 ± 0.09
s_3	1 ± 0.2	1.0 ± 0.3	1.0 ± 0.3	1.0 ± 0.3
a_o	$(1.3 \pm 0.2) \times 10^{-8}$	$(6 \pm 2) \times 10^{-9}$	$(4 \pm 1) \times 10^{-9}$	$(1.8 \pm 0.3) \times 10^{-8}$
p	-3.87 ± 0.03	-3.72 ± 0.07	-3.82 ± 0.06	-3.53 ± 0.04
b_o	$(3.06 \pm 0.03) \times 10^{-3}$	$0.00243 \pm 5.00E-05$	$(2.59 \pm 0.05) \times 10^{-3}$	$(2.3 \pm 0.1) \times 10^{-3}$

Table S6: Fit parameters for HMT-PMBI(I^-), ambient conditions.

	97.5% dm	89.7% dm	80.2% dm
a_1	$(3.5 \pm 0.5) \times 10^{-4}$	$(2.4 \pm 0.2) \times 10^{-4}$	$(1.55 \pm 0.08) \times 10^{-4}$
b_1	0.40 ± 0.03	0.389 ± 0.005	0.356 ± 0.002
c_1	0.19 ± 0.04	0.20 ± 0.03	0.18 ± 0.02
s_1	0.7 ± 0.3	0.9 ± 0.4	0.9 ± 0.2
a_2	$(2.4 \pm 0.3) \times 10^{-3}$	$(1.88 \pm 0.03) \times 10^{-3}$	$(1.23 \pm 0.01) \times 10^{-3}$
b_2	1.222 ± 0.005	1.209 ± 0.002	1.148 ± 0.003
c_2	0.52 ± 0.04	0.544 ± 0.007	0.533 ± 0.004
s_2	0.5 ± 0.1	0.53 ± 0.05	0.75 ± 0.03
a_3	$(3.9 \pm 0.1) \times 10^{-3}$	$(2.44 \pm 0.03) \times 10^{-3}$	$(7.74 \pm 0.09) \times 10^{-4}$
b_3	1.851 ± 0.008	1.796 ± 0.004	1.735 ± 0.004
c_3	1.2 ± 0.2	1.00 ± 0.02	0.64 ± 0.01
s_3	0 ± 0.2	0.00 ± 0.03	1.00 ± 0.05
a_o	$(1.0 \pm 0.4) \times 10^{-9}$	$(1.0 \pm 0.4) \times 10^{-9}$	$(1.00 \pm 0.06) \times 10^{-9}$
p	-3.63 ± 0.06	-3.65 ± 0.06	-3.86 ± 0.01
b_o	$(1.5 \pm 0.3) \times 10^{-3}$	$(1.69 \pm 0.04) \times 10^{-3}$	$(2.19 \pm 0.01) \times 10^{-4}$

Table S7: Fit parameters for HMT-PMBI(Cl^-), ambient conditions.

	97.5% dm	89.7% dm	80.2% dm
a_1	$(2 \pm 2) \times 10^{-4}$	$(1.5 \pm 0.8) \times 10^{-4}$	$(1.9 \pm 0.7) \times 10^{-4}$
b_1	0.35 ± 0.04	0.33 ± 0.03	0.33 ± 0.04
c_1	0.1 ± 0.2	0.58 ± 0.05	0.14 ± 0.02
s_1	1 ± 0.5	0.0 ± 0.3	1.0 ± 0.4
a_2	$(3.9 \pm 0.1) \times 10^{-3}$	$(4.3 \pm 0.1) \times 10^{-4}$	$(3.9 \pm 0.4) \times 10^{-4}$
b_2	1.164 ± 0.005	1.107 ± 0.002	1.070 ± 0.002
c_2	0.74 ± 0.03	0.78 ± 0.02	0.703 ± 0.006
s_2	0.2 ± 0.1	0.62 ± 0.07	0.59 ± 0.05
a_3	$(2.8 \pm 0.3) \times 10^{-3}$	$(3.1 \pm 0.1) \times 10^{-4}$	$(2.3 \pm 0.2) \times 10^{-4}$
b_3	1.880 ± 0.006	1.882 ± 0.004	1.859 ± 0.003
c_3	0.69 ± 0.05	0.707 ± 0.008	0.707 ± 0.009
s_3	1 ± 0.2	1.00 ± 0.02	0.88 ± 0.07
a_o	$(2.2 \pm 0.4) \times 10^{-8}$	$(2.40 \pm 0.07) \times 10^{-4}$	$(1.0 \pm 0.2) \times 10^{-8}$
p	-3.44 ± 0.03	-3.26 ± 0.03	-3.62 ± 0.04
b_o	$(2.6 \pm 0.2) \times 10^{-3}$	$(1.00 \pm 0.06) \times 10^{-3}$	$(2.96 \pm 0.04 \times 10^{-3}$

Table S8: Fit parameters for HMT-PMBI(I^-), after soaking.

	97.5% dm	89.7% dm	80.2% dm
a_1	$(3.4 \pm 0.3) \times 10^{-4}$	$(3 \pm 2) \times 10^{-4}$	$(1.5 \pm 0.1) \times 10^{-4}$
b_1	0.379 ± 0.003	0.39 ± 0.02	0.365 ± 0.004
c_1	0.15 ± 0.01	0.3 ± 0.4	0.29 ± 0.02
s_1	1.0 ± 0.3	0 ± 0.3	0.0 ± 0.2
a_2	$(2.43 \pm 0.05) \times 10^{-3}$	$(1.3 \pm 0.1) \times 10^{-3}$	$(9 \pm 1) \times 10^{-4}$
b_2	1.215 ± 0.002	1.222 ± 0.005	1.17 ± 0.02
c_2	0.473 ± 0.007	0.53 ± 0.03	0.57 ± 0.04
s_2	1.00 ± 0.05	0.7 ± 0.2	0.66 ± 0.09
a_3	$(5.45 \pm .06) \times 10^{-3}$	$(2.9 \pm 0.2) \times 10^{-3}$	$(4.4 \pm 0.2) \times 10^{-4}$
b_3	1.827 ± 0.003	1.882 ± 0.009	1.76 ± 0.06
c_3	1.06 ± 0.02	1.05 ± 0.05	0.6 ± 0.1
s_3	0.04 ± 0.05	0.0 ± 0.2	1.00 ± 0.05
a_o	$(5.4 \pm 0.3) \times 10^{-7}$	$(3.4 \pm 0.5) \times 10^{-9}$	$(2.8 \pm 0.3) \times 10^{-9}$
p	-3.05 ± 0.01	-3.60 ± 0.03	-3.62 ± 0.02
b_o	$(1.39 \pm 0.05) \times 10^{-3}$	$(2.3 \pm 0.3) \times 10^{-3}$	$(1.71 \pm 0.01) \times 10^{-4}$

Table S9: Fit parameters for HMT-PMBI(Cl^-), after soaking.

	97.5% dm	89.7% dm	80.2% dm
a_1			$(1 \pm 1) \times 10^{-4}$
b_1			0.2 ± 0.1
c_1			4 ± 2
s_1			0.6 ± 0.4
a_2	$(2.72 \pm 0.08) \times 10^{-3}$	$(4.1 \pm 0.2) \times 10^{-3}$	$(2.58 \pm 0.07) \times 10^{-3}$
b_2	1.124 ± 0.003	1.127 ± 0.008	1.091 ± 0.002
c_2	0.509 ± 0.008	0.57 ± 0.01	0.70 ± 0.02
s_2	1.00 ± 0.08	1.00 ± 0.04	0.2 ± 0.1
a_3	$(8.2 \pm 0.1) \times 10^{-3}$	$(7.9 \pm 0.1) \times 10^{-3}$	$(3.0 \pm 0.1) \times 10^{-3}$
b_3	1.889 ± 0.002	1.878 ± 0.003	1.859 ± 0.004
c_3	0.78 ± 0.01	0.71 ± 0.03	0.78 ± 0.03
s_3	0 ± 0.08	0.6 ± 0.2	0.10 ± 0.09
a_o	$(8.2 \pm 0.9) \times 10^{-4}$	$(1.1 \pm 0.3) \times 10^{-5}$	$(4 \pm 2) \times 10^{-3}$
p	-0.82 ± 0.04	-1.82 ± 0.06	-3.66 ± 0.09
b_o	$(1.4 \pm 0.2) \times 10^{-3}$	0.0021 ± 0.0001	$(2.5 \pm 0.1) \times 10^{-3}$

Table S10: Length scales corresponding to each peak position, vacuum.

Sample	MAXS Peak (Å)	Peak 1 (Å)	Peak 2 (Å)
97.5% dm HMT-PMBI(I^-)	17.9 ± 0.1	$5.62 \pm .01$	$3.65 \pm .01$
89.7% dm HMT-PMBI(I^-)	18.0 ± 0.2	$5.73 \pm .01$	$3.74 \pm .02$
80.2% dm HMT-PMBI(I^-)	18.9 ± 0.2	$5.81 \pm .02$	$3.70 \pm .03$
65.9% dm HMT-PMBI(I^-)	20.2 ± 0.5	$6.05 \pm .02$	$3.91 \pm .02$
97.5% dm HMT-PMBI(Cl^-)	18.4 ± 0.1	$6.00 \pm .01$	$3.78 \pm .02$
89.7% dm HMT-PMBI(Cl^-)	19.9 ± 0.2	$6.37 \pm .01$	$3.80 \pm .02$
80.2% dm HMT-PMBI(Cl^-)	20.0 ± 0.2	$6.47 \pm .02$	$3.86 \pm .02$
65.9% dm HMT-PMBI(Cl^-)	21.9 ± 0.3	$6.51 \pm .02$	$3.93 \pm .02$

Table S11: Length scales corresponding to each peak position, ambient.

Sample	MAXS Peak (Å)	Peak 1 (Å)	Peak 2 (Å)
97.5% dm HMT-PMBI(I^-)	19 ± 2	$6.27 \pm .03$	$4.14 \pm .02$
89.7% dm HMT-PMBI(I^-)	$19.7 \pm .3$	$6.34 \pm .01$	$4.27 \pm .01$
80.2% dm HMT-PMBI(I^-)	$21.5 \pm .1$	$6.68 \pm .02$	$4.42 \pm .02$
97.5% dm HMT-PMBI(Cl^-)	22 ± 3	$6.59 \pm .03$	$4.08 \pm .01$
89.7% dm HMT-PMBI(Cl^-)	23 ± 2	$6.92 \pm .01$	$4.07 \pm .01$
80.2% dm HMT-PMBI(Cl^-)	23 ± 3	$7.16 \pm .01$	$4.12 \pm .01$

Table S12: Length scales corresponding to each peak position, soaked.

Sample	MAXS Peak (Å)	Peak 1 (Å)	Peak 2 (Å)
97.5% dm HMT-PMBI(I^-)	$20.2 \pm .2$	$6.31 \pm .01$	$4.20 \pm .01$
89.7% dm HMT-PMBI(I^-)	20 ± 1	$6.27 \pm .03$	$4.07 \pm .02$
80.2% dm HMT-PMBI(I^-)	$21.0 \pm .2$	$6.6 \pm .1$	$4.4 \pm .2$
97.5% dm HMT-PMBI(Cl^-)		$6.82 \pm .02$	$4.06 \pm .01$
89.7% dm HMT-PMBI(Cl^-)		$6.80 \pm .05$	$4.08 \pm .01$
80.2% dm HMT-PMBI(Cl^-)	40 ± 40	$7.03 \pm .01$	$4.12 \pm .01$